

Supplementary Information for:

Properties of NaPF₆ Electrolytes and Effect of Electrolyte Concentration on Performance in Sodium-Ion Batteries

Darren M. C. Ould,^[a,b] Stefan Oswald,^[a,b] Holly E. Smith,^[a] Christopher A. O’Keefe,^[a] Tengfei Song,^[b,c] Emma Kendrick,^[b,c] Dominic S. Wright^[a,b] and Clare P. Grey^{*[a,b]}

[a] Yusuf Hamied Department of Chemistry, University of Cambridge, Lensfield Road, Cambridge, CB2 1EW, U.K.

[b] The Faraday Institution, Quad One, Harwell Science and Innovation Campus, Didcot, OX11 0RA, U.K.

[c] School of Metallurgy and Materials, University of Birmingham, Birmingham B15 2TT, UK.

Contents

S1 Electrolyte preparation	2
S2 Electrochemistry experimental	2
S3 DOSY NMR spectroscopy	4
S4 Viscosity measurements	6
S5 Cycling plots	8
S6 Scanning electron microscopy (SEM) images of electrodes	11
S7 NMR Spectroscopy	13

S1 Electrolyte preparation

Five electrolyte solutions of NaPF_6 in EC:DEC (1:1 v/v) (0.25 M, 0.5 M, 1 M, 1.5 M and 2 M) were prepared in an argon-filled glovebox by dissolving the required amount of salt in the binary carbonate solvent blend. The electrolyte solutions were stored in aluminium bottles that were dried at 80°C for six hours. Karl-Fischer measurements were recorded on the electrolyte solutions, which typically gave values in the range of 30–50 ppm water concentration. Solution-state ^1H and ^{19}F NMR spectroscopy was performed to assess the quality of the electrolytes before using them.

S2 Electrochemistry experimental

S2.1 Bulk conductivity measurements

Solution conductivity measurements were made in a TSC 70 Closed cell from RHD instruments. $70\ \mu\text{l}$ of each liquid was filled into the cell and sealed inside an argon-filled glovebox. Impedance spectra were measured using a PalmSens4 or Biologic potentiostat, with an applied voltage amplitude of 10 mV and frequencies between 1 MHz and 1 Hz. The impedance spectra were fitted using the equivalence circuit R+Q, and the solution conductivity at 25°C was found by taking the reciprocal of the R component, multiplied by the cell constant.

The cell constant was determined using a $1413\ \mu\text{S cm}^{-1}$ conductivity standard solution from Hanna Instruments. $70\ \mu\text{l}$ of the solution was filled into the cell, which was sealed and placed in an incubator held at 25°C . An impedance spectrum was measured as above. The spectrum was fitted with a Q+R/Q circuit and the measured resistance was multiplied by $1413\ \mu\text{S cm}^{-1}$ to determine the cell constant, which was found to be $6.1 \pm 0.1\ \text{cm}^{-1}$.

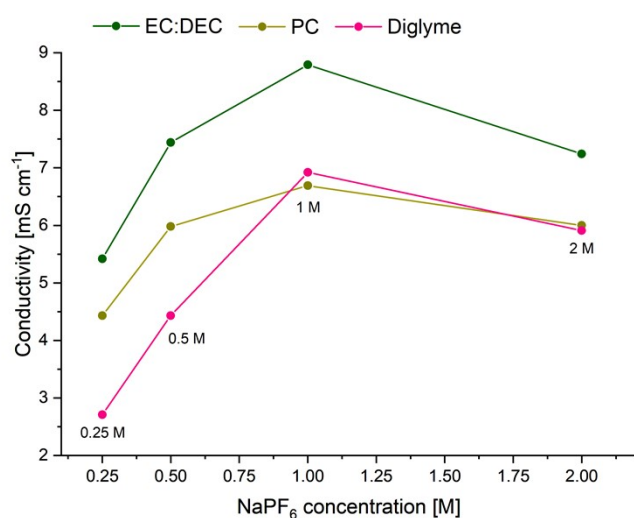


Figure S1 Bulk conductivity of 0.25 M, 0.5 M, 1 M and 2 M NaPF_6 electrolytes in EC:DEC (1:1 v/v) (green), PC (yellow) and diglyme (pink) solvents. Measured at 25°C .

S2.2 Coin cell preparation

Coin cells (2032 from Cambridge energy solutions) were prepared in an argon glovebox ($O_2 < 1$ ppm, $H_2O < 1$ ppm). For Na-ion battery cells, 2-electrode single-layer coin cells with 1.54 cm^2 cathode area were assembled with a geometrically over-sized hard-carbon anode (1.77 cm^2). The $NaNi_{0.33}Fe_{0.33}Mn_{0.33}O_2$ (NFM111) cathode material was supplied by Jiangsu Xiangying New Energy Technology Co. China, and the anode hard carbon used for this study was a Kuranode type 1 purchased from Kuraray Co. Ltd. The cathode electrode was prepared by mixing 88% NFM, 5.8% carbon black (C65, TimCal), 0.2% multiwalled carbon nanotubes (MWCNT), 1% oxalic acid additive, and 5% polyvinylidene fluoride (PVDF 5130, Solvay) in N-methyl-2-pyrrolidone (NMP) solvent. The anode electrode was prepared by mixing 96% HC, 1% carbon black (C45, Timcal), 1% carboxymethyl cellulose (CMC) (BVH8, Ashland) and 2% styrene-butadiene rubber (SBR) (BM-451B, Zeon) in water. The mixing was processed in a Thinky ARE-250 planetary mixer. The capacity ratio between the anode and cathode was 1.2:1. The porosity of the cathode and anode electrode was calendared to be around 35% and 30%, respectively. The thickness of the cathode is approximately $50\text{ }\mu\text{m}$, the thickness of the anode is approximately $65\text{ }\mu\text{m}$.

The electrodes were dried at 110°C under vacuum (1×10^{-2} mbar) for 18 hours before using. Glass fibre, which was dried under vacuum (1×10^{-2} mbar) at 100°C for 18 hours, was used as the separator, with $100\text{ }\mu\text{l}$ of electrolyte.

Na-ion coin cells were tested either at room-temperature (20°C and 21°C) or 50°C with a battery cycler (Arbin LTB or LAND CT2001A cycler brands). The formation protocol consisted of 2 charge-discharge cycles at a rate of C/20 between a voltage limit of 4.0–1.5 V. For cycle life tests, two different protocols were used. The first protocol involved two C/20 formation cycles, followed by two 2C and 46 C/2 cycles. This set of cycles was then repeated six times, giving a total of 300 cycles. The second protocol involved two C/20 formation cycles, followed by C/2 cycles for both charge and discharge. This method was applied at either 20°C or 50°C to assess the effects of temperature on cycling.

S3 DOSY NMR spectroscopy

Solution NMR experiments were conducted on a Bruker 11.7 T magnet ($\nu_0(^1\text{H}) = 500.20$ MHz, $\nu_0(^{19}\text{F}) = 470.62$ MHz) equipped with an Avance IIIHD console. A 5 mm BBO probe was used for all experiments. Diffusion coefficients were measured using a bipolar pulsed gradient stimulated echo experiment with spoil gradients. Diffusion times were 10 ms and gradient pulse lengths of 1.2 ms and 2.5 ms were used for ^1H and ^{19}F , respectively. The gradient strengths were varied and the diffusion coefficients were determined by fitting the signal decay using the Stejskal-Tanner equation.

Table S1: Diffusion coefficients of ethylene carbonate (EC), diethyl carbonate (DEC) and PF_6^- anion.

Concentration (M)	D_{EC}	$D_{\text{DEC (ethyl)}}$	$D_{\text{DEC (methyl)}}$	$D_{\text{PF}_6^-}$	$D_{\text{EC}}/D_{\text{PF}_6^-}$
0.25	7.18	6.38	6.44	4.61	1.56
0.5	5.72	5.91	5.82	3.22	1.79
1	3.29	3.61	3.52	2.67	1.23
1.5	2.24	2.39	2.31	1.43	1.57
2	1.87	2.05	1.96	1.25	1.50

Measured by ^1H or ^{19}F DOSY NMR spectroscopy. Diffusion coefficients in units of $10^{-10} \text{ m}^2 \text{ s}^{-1}$.

Table S2: Diffusion coefficients of PF_6^- anion measured by ^{19}F DOSY NMR spectroscopy. Diffusion

Electrolyte	$D_{\text{PF}_6^-}$
1 M NaPF_6 in EC:DEC	2.67
1 M NaPF_6 in PC	1.49
1 M NaPF_6 in diglyme	2.51

coefficients in units of $10^{-10} \text{ m}^2 \text{ s}^{-1}$. Electrolyte is 1 M NaPF_6 in either EC:DEC (1:1 v/v), PC or diglyme solvents.

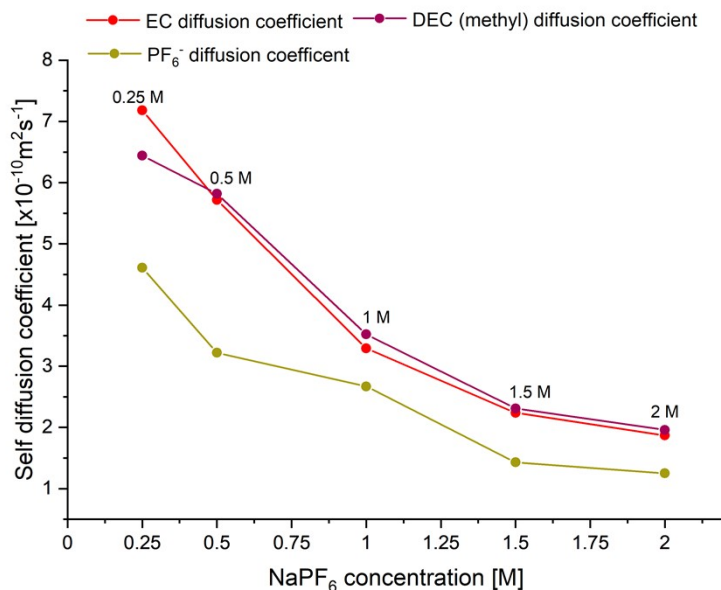


Figure S2 Self-diffusion coefficients of the EC solvent molecule (red) (from ^1H DOSY NMR), DEC solvent molecule (from ^1H DOSY NMR, methyl group) and PF_6^- anion (yellow) (from ^{19}F DOSY NMR) of 0.25 M, 0.5 M, 1 M, 1.5 M and 2 M NaPF_6 in EC:DEC (1:1 v/v) electrolytes.

As described in the manuscript, if we assume 4 EC solvent molecules are coordinated to the Na^+ cation at all electrolyte concentrations, then the percentage of free EC solvent molecules (not coordinated to Na^+) decreases from 87% in the 0.25 M NaPF_6 electrolyte, 73% in the 0.5 M NaPF_6 electrolyte, 47% in the 1 M NaPF_6 sample and 20% in the 1.5 M NaPF_6 sample. All the EC molecules would be coordinated to Na^+ .

If the amount of coordinated EC solvent molecules is lower and we assume that 3 EC solvent molecules are coordinated to the Na^+ cation at all electrolyte concentrations, then the percentage of free EC solvent molecules (not coordinated to Na^+) decreases from 90% in the 0.25 M NaPF_6 electrolyte, 80% in the 0.5 M NaPF_6 electrolyte, 60% in the 1 M NaPF_6 sample and 40% in the 1.5 M NaPF_6 sample. 20% of the EC molecules will be free (not coordinated to Na^+) in the 2 M NaPF_6 electrolyte.

S4 Viscosity measurements

S4.1 Viscosity measurements

Kinematic viscosities were measured in an argon glovebox with a Micro-Ostwald viscometer, type 51610/I (SI Analytics), with an instrument constant $K = 0.01063 \text{ mm}^2 \text{ s}^{-2}$. 2 ml of the liquid was filled into the viscometer, and the time taken to fall was measured three times and averaged. The temperature inside the glovebox was approximately 25°C. Kinematic viscosities were converted to dynamic viscosities by multiplying by liquid density; the density was measured by weighing 1 ml of liquid in an argon glovebox.



Figure S3: Photographs showing the Micro-Ostwald viscometer used to determine the viscosity of NaPF_6 electrolyte solutions.

S4.2 Viscosity results

Concentration (M)	Dynamic viscosity (cP)
0.25	1.9
0.5	2.6
1	3.9
1.5	6.2
2	10.4

Table S3: Dynamic viscosity of 0.25 M, 0.5 M, 1 M and 2 M NaPF_6 concentration in EC:DEC (1:1 v/v).

S4.3 Walden plot

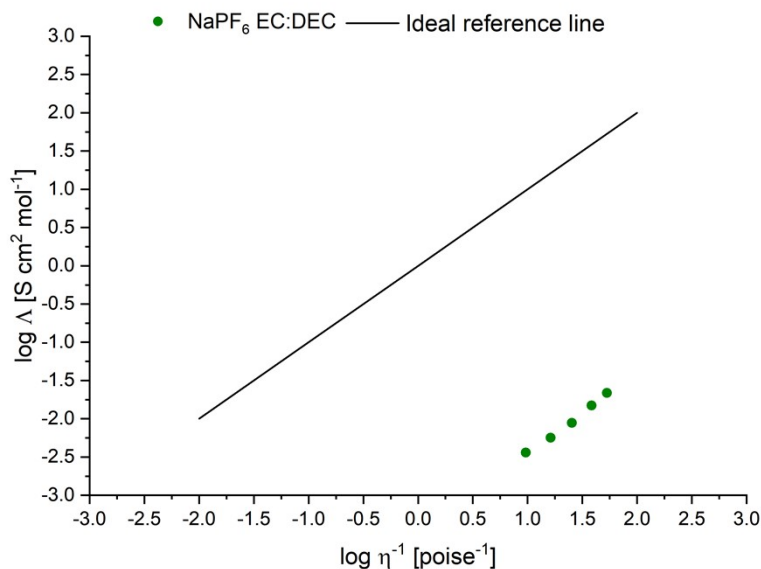


Figure S4: Walden plot of the \log_{10} of molar conductivity against the \log_{10} of reciprocal viscosity. Electrolyte is 0.25 M, 0.5 M, 1 M, 1.5 M and 2 M NaPF₆ in EC:DEC (1:1 v/v), measured at 25°C. Reference line of unit gradient represents a fully dissociated salt (aqueous 1 M KCl).

The ionicity of a salt can be determined from a Walden plot using the equation (D. Monti, E. Jónsson, A. Boschini, M. R. Palacín, A. Ponrouch and P. Johansson, *Phys. Chem. Chem. Phys.*, 2020, **22**, 22768–22777):

$$\%ionicity = 10^{-\Delta W} \times 100\%$$

Where: ΔW = the vertical distance measured between the reference line and the tested electrolyte.

The vertical distances between the different NaPF₆ electrolyte concentrations and the reference line are approximately the same for all concentrations tested at 25°C. Thus, suggesting the ionicity does not significantly change with the concentrations tested.

S5 Cycling plots

S5.1 Sodium half cells

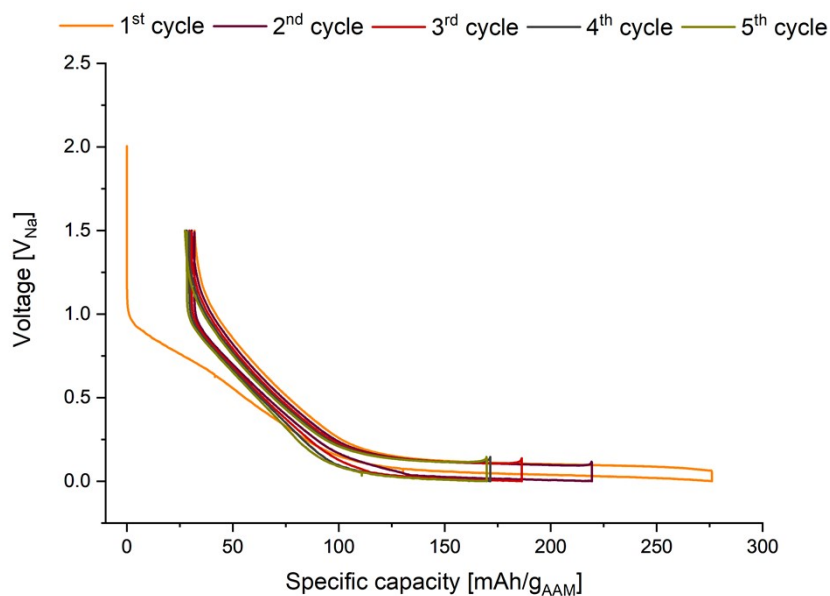


Figure S5: Voltage vs. specific capacity, normalized by the mass of anode active material (AAM). Hard-carbon anode in a coin half-cell vs. sodium metal with 100 μ l of 1 M $NaPF_6$ in EC:DEC (1:1 v/v) as electrolyte. The cell was cycled five times at C/10 between 0.01 and 2.0 V_{Na} at 21°C.

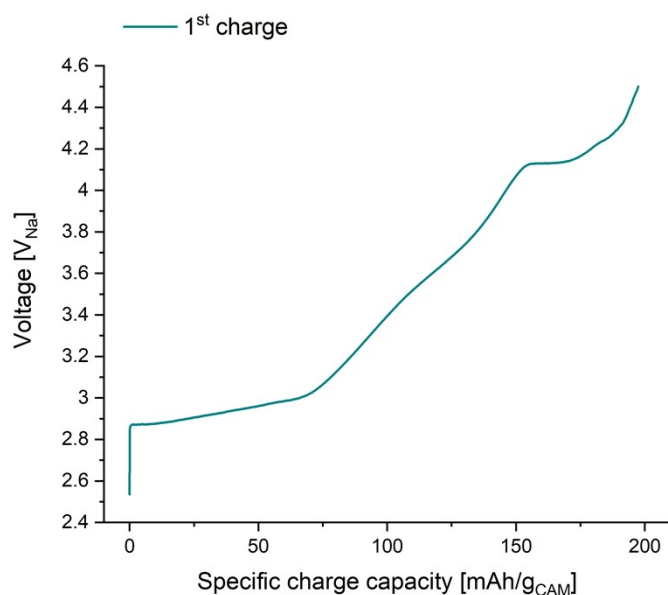


Figure S6: Voltage vs. specific charge capacity, normalized by the mass of cathode active material (CAM). $NaNi_{0.33}Fe_{0.33}Mn_{0.33}O_2$ cathode in a coin half-cell vs. sodium metal with 100 μ l of 1 M $NaPF_6$ in EC:DEC (1:1 v/v) as electrolyte. The cell was charged at C/10 to 4.5 V_{Na} at 21°C.

S5.2 C/2 rate cycling plots

Room-temperature cycling (20°C)

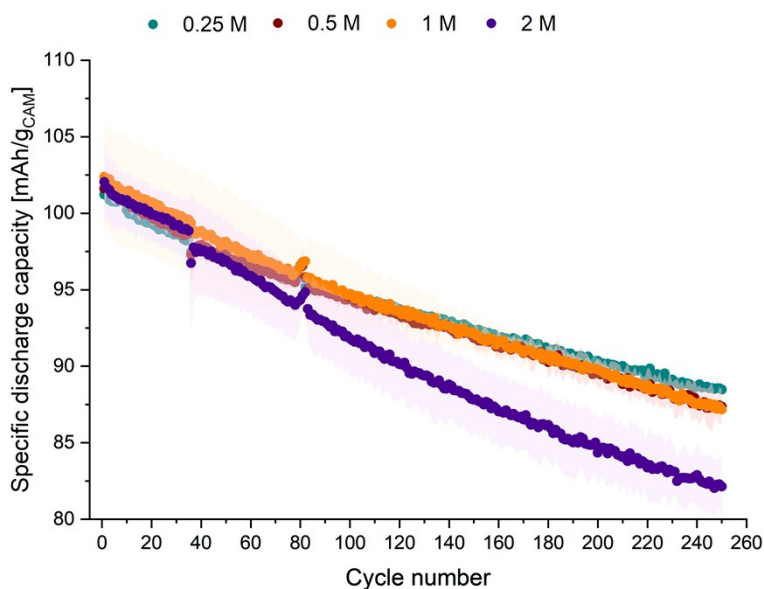


Figure S7: Specific discharge capacity vs. cycle number using NFM111 cathode and hard-carbon anode. C/2 C-rate based on the expected capacity of 138 mAh g⁻¹ of the cathode, using cell voltage limits of 1.5 and 4.0 V. Electrolyte is 0.25 M (green), 0.5 M (red), 1 M (orange) and 2 M (purple) NaPF₆ in EC:DEC (1:1 v/v). Error bars display standard deviation of 2-coin cells; cycled at 20°C.

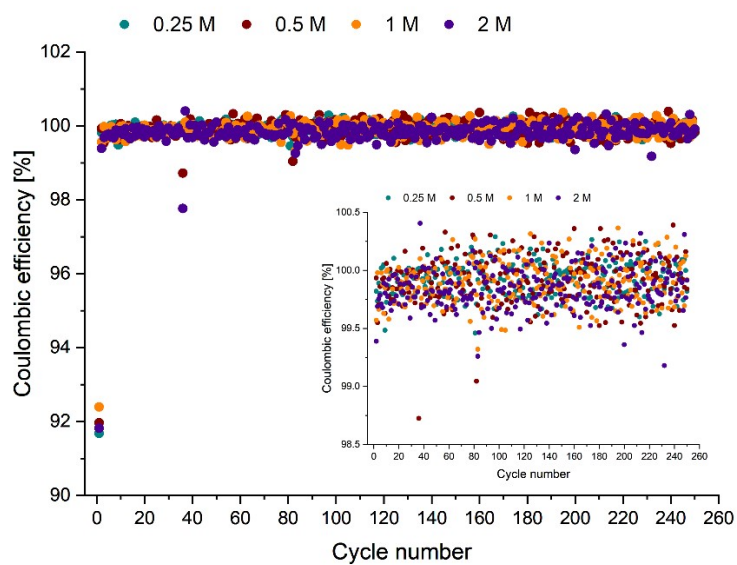


Figure S8: Coulombic efficiency vs. cycle number using NFM111 cathode and hard-carbon anode. C/2 C-rate based on the expected capacity of 138 mAh g⁻¹ of the cathode, using cell voltage limits of 1.5

and 4.0 V. Electrolyte is 0.25 M (green), 0.5 M (red), 1 M (orange) and 2 M (purple) NaPF₆ in EC:DEC (1:1 v/v). Averaged from 2-coin cells; cycled at 20°C.

50°C temperature cycling

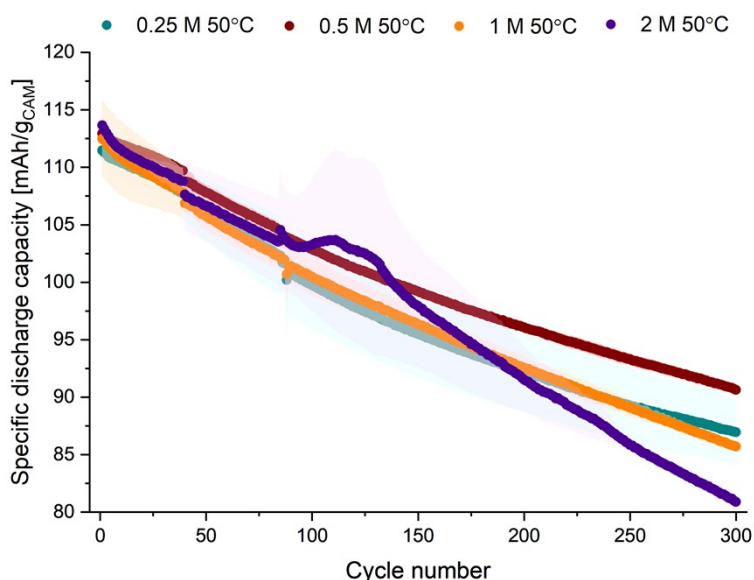


Figure S9: Specific discharge capacity vs. cycle number using NFM111 cathode and hard-carbon anode. C/2 C-rate based on the expected capacity of 138 mAh g⁻¹ of the cathode, using cell voltage limits of 1.5 and 4.0 V. Electrolyte is 0.25 M (green), 0.5 M (red), 1 M (orange) and 2 M (purple) NaPF₆ in EC:DEC (1:1 v/v). Error bars display standard deviation of 2-coin cells; cycled at 50°C.

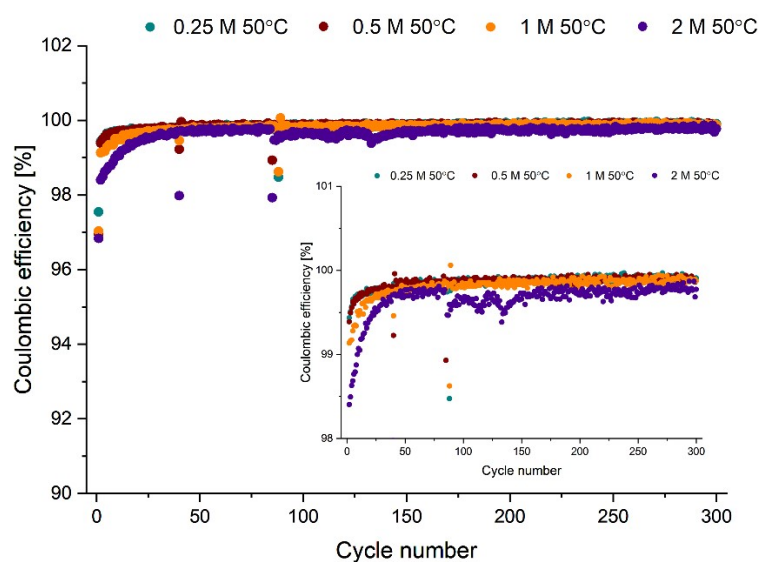


Figure S10: Coulombic efficiency vs. cycle number using NFM111 cathode and hard-carbon anode. C/2 C-rate based on the expected capacity of 138 mAh g⁻¹ of the cathode, using cell voltage limits of 1.5

and 4.0 V. Electrolyte is 0.25 M (green), 0.5 M (red), 1 M (orange) and 2 M (purple) NaPF₆ in EC:DEC (1:1 v/v). Averaged from 2-coin cells; cycled at 50°C.

S6 Scanning electron microscopy (SEM) images of electrodes

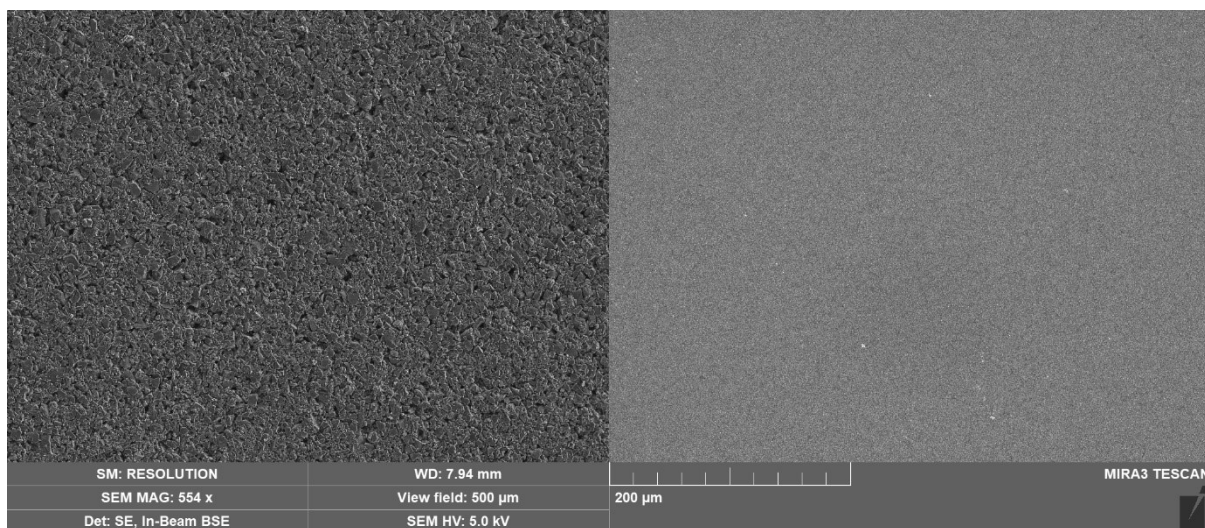


Figure S11: SEM image of pristine hard-carbon anode.

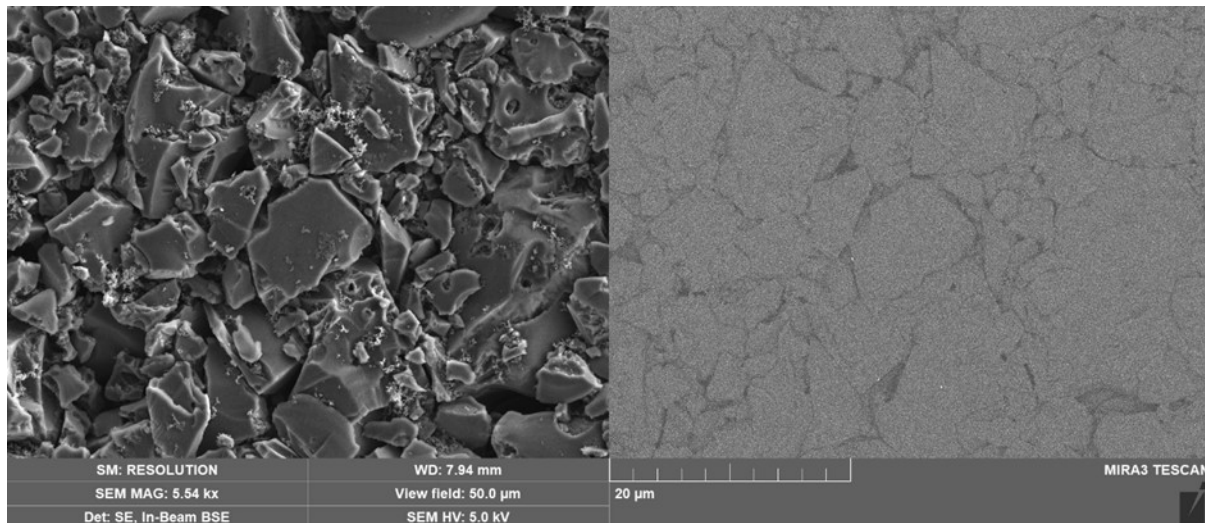


Figure S12: SEM image of pristine hard-carbon anode.

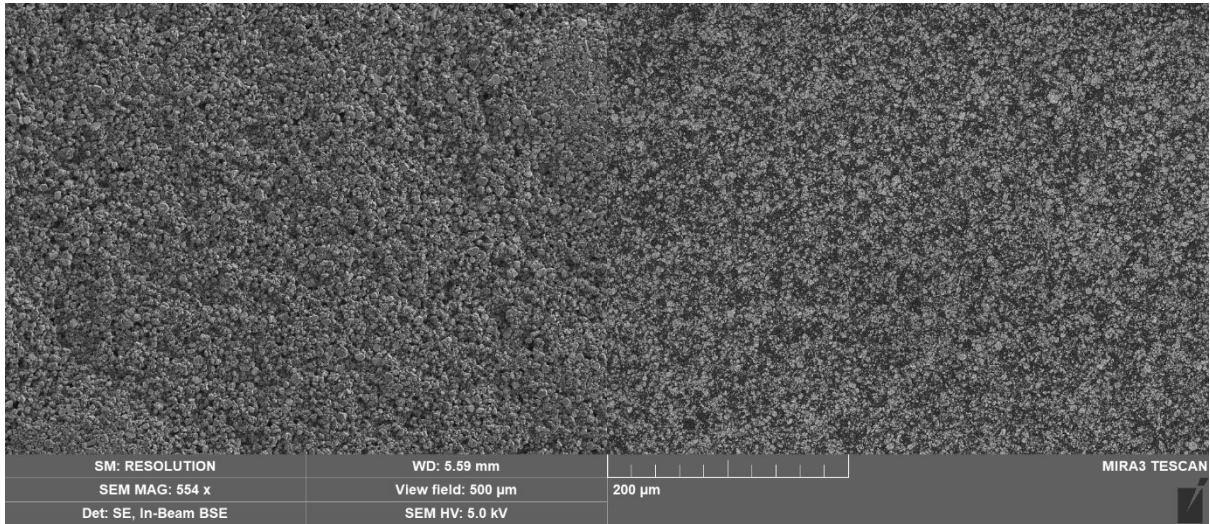


Figure S13: SEM image of pristine cathode ($\text{NaNi}_{0.33}\text{Fe}_{0.33}\text{Mn}_{0.33}\text{O}_2$).

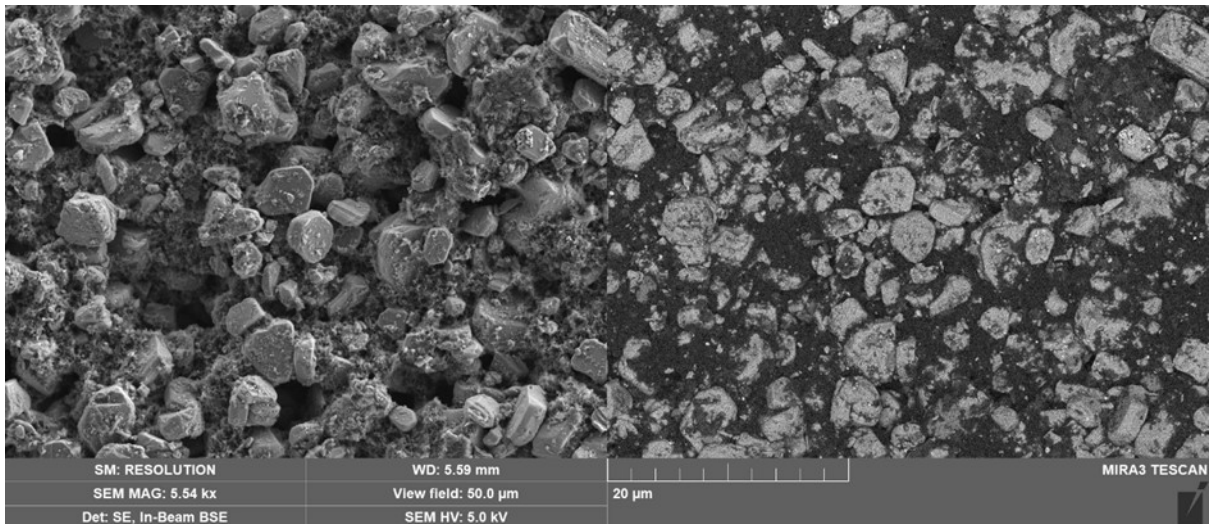


Figure S14: SEM image of pristine cathode ($\text{NaNi}_{0.33}\text{Fe}_{0.33}\text{Mn}_{0.33}\text{O}_2$).

S7 NMR Spectroscopy

Figure S15 ^1H NMR (500 MHz, 295 K) spectrum of 0.25 M NaPF_6 in EC:DEC (1:1 v/v).

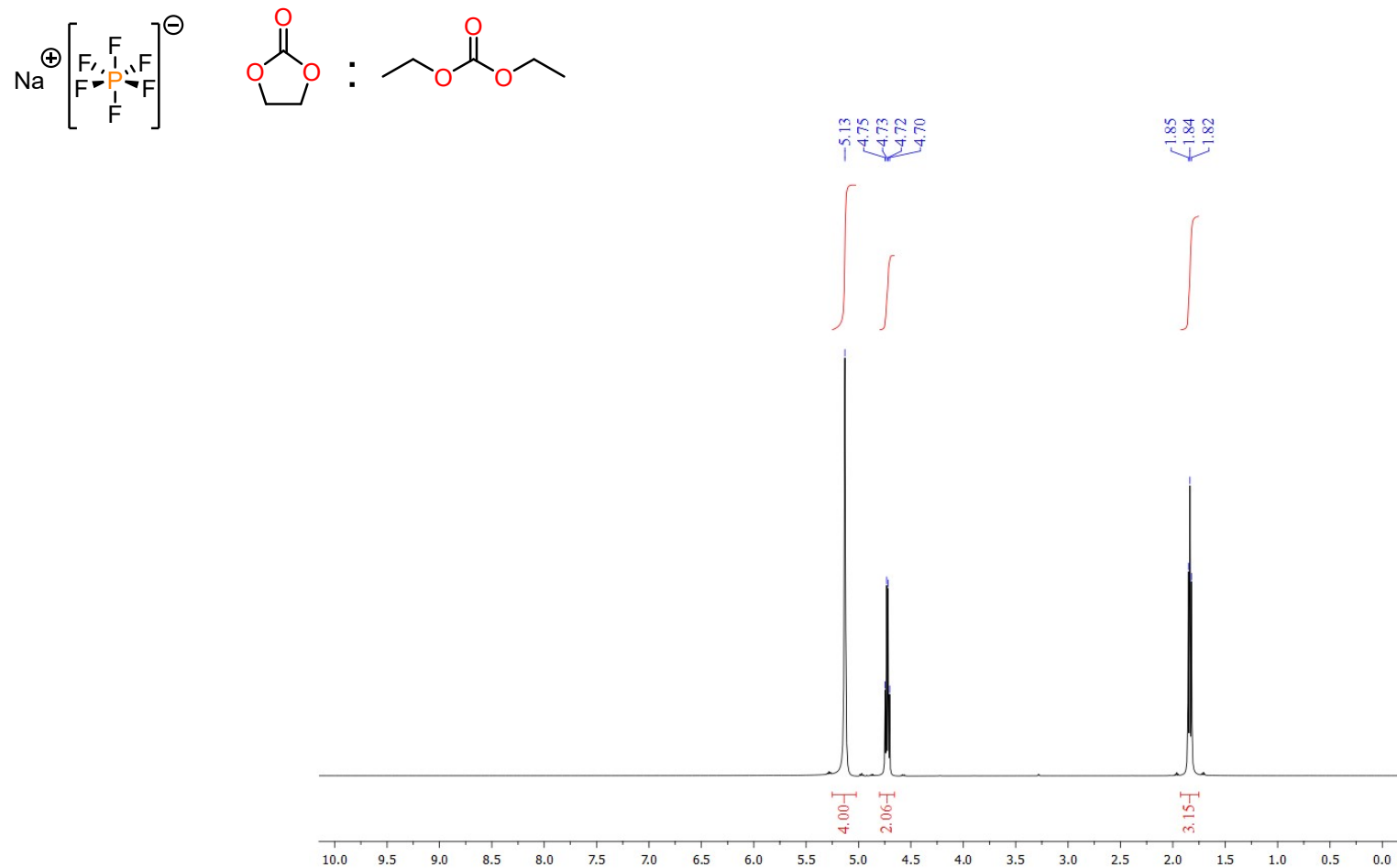


Figure S16 ^{19}F NMR (471 MHz, 295 K) spectrum of 0.25 M NaPF_6 in EC:DEC (1:1 v/v).

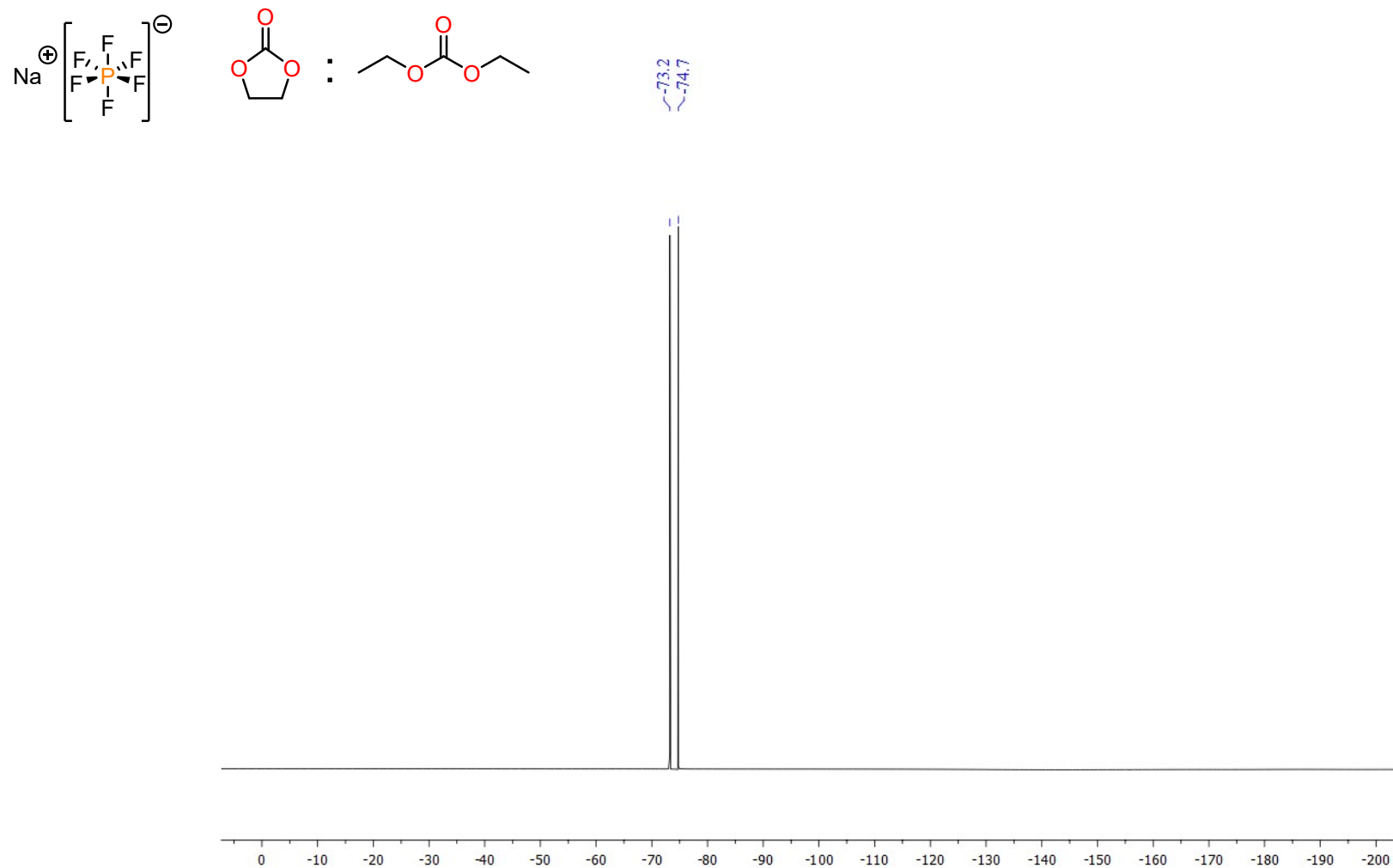


Figure S17 ^1H NMR (500 MHz, 295 K) spectrum of 0.5 M NaPF_6 in EC:DEC (1:1 v/v).

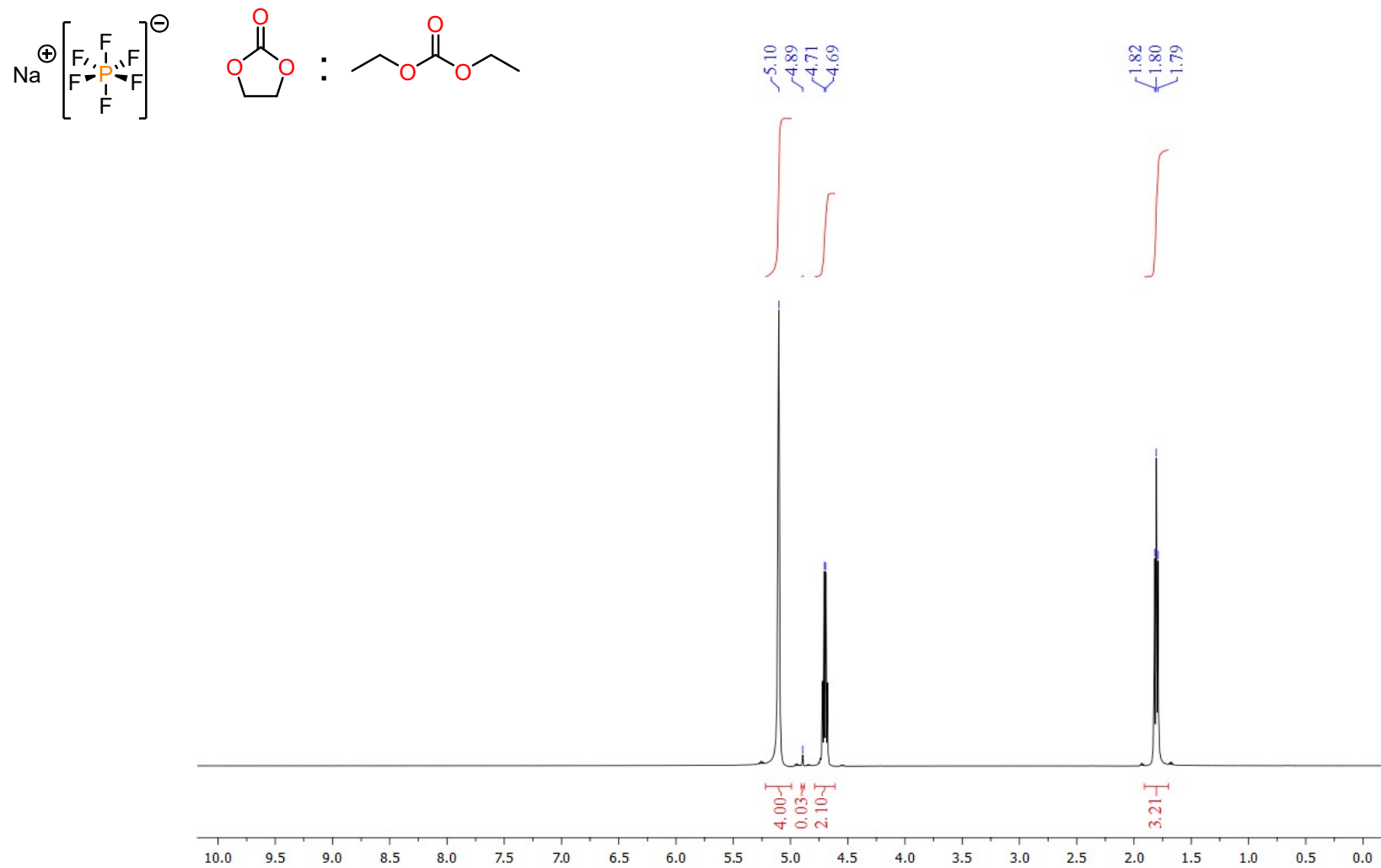


Figure S18 ^{19}F NMR (471 MHz, 295 K) spectrum of 0.5 M NaPF_6 in EC:DEC (1:1 v/v).



Figure S19 ^1H NMR (500 MHz, 295 K) spectrum of 1 M NaPF_6 in EC:DEC (1:1 v/v).

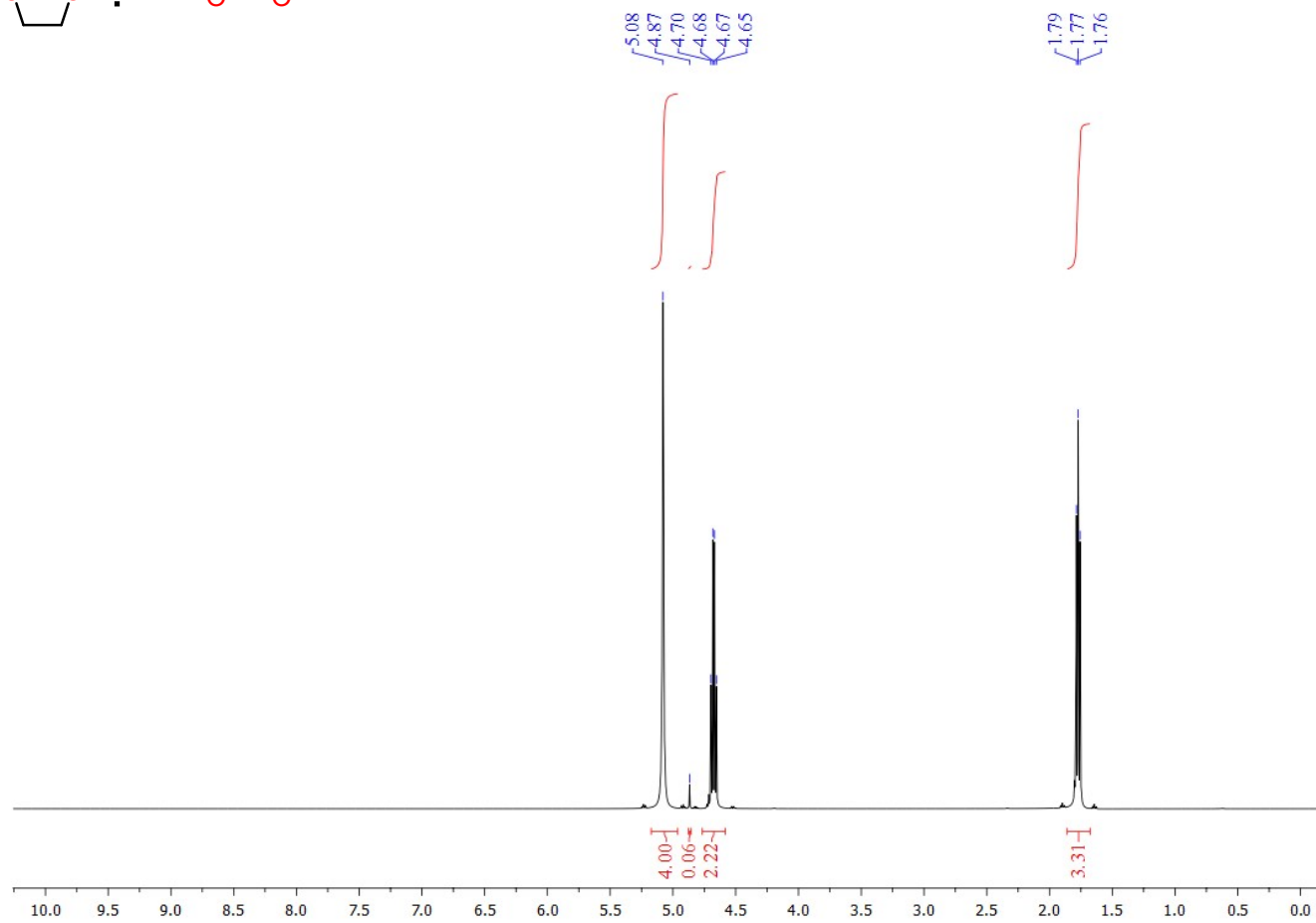
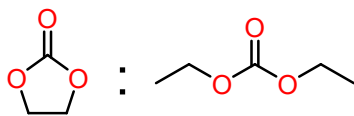
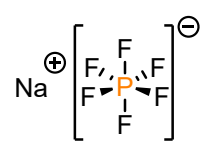


Figure S20 ^{19}F NMR (471 MHz, 295 K) spectrum of 1 M NaPF_6 in EC:DEC (1:1 v/v).



Figure S21 ^1H NMR (500 MHz, 295 K) spectrum of 2 M NaPF_6 in EC:DEC (1:1 v/v).

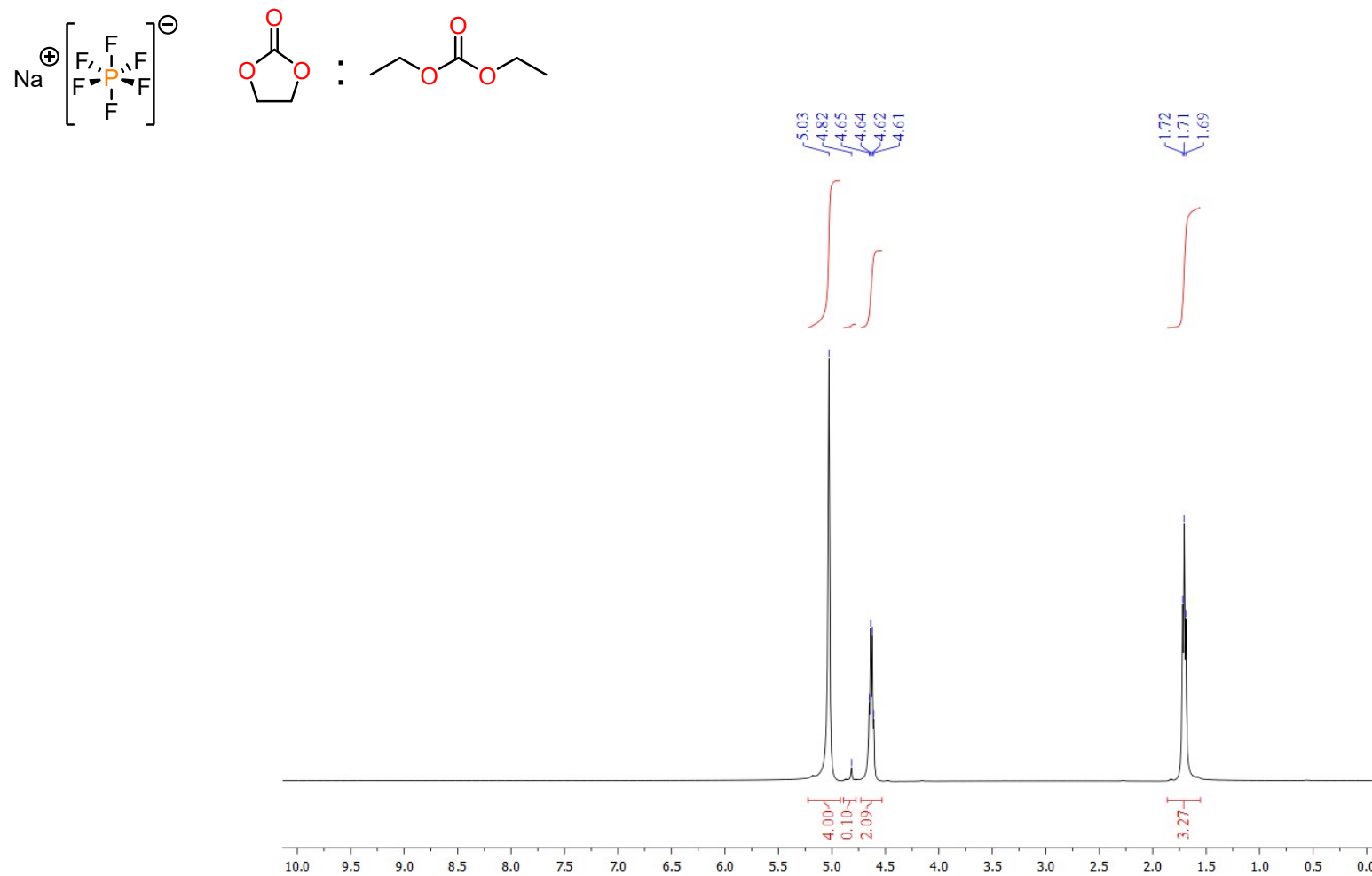


Figure S22 ^{19}F NMR (471 MHz, 295 K) spectrum of 2 M NaPF_6 in EC:DEC (1:1 v/v).

